Materials Science and Engineering B 285 (2022) 115937

Contents lists available at ScienceDirect

Materials Science & Engineering B

journal homepage: www.elsevier.com/locate/mseb

Carbon nanotubes based multi-directional strain sensor

A. Santos [a,*], L. Amorim [a,b], J.P. Nunes [a], A.F. Silva [c], J.C. Viana [a]

[a] IPC/LASI – Institute for Polymers and Composites/Associated Laboratory in Intelligent Systems, University of Minho, Guimarães, Portugal
[b] INEGI – Instituto de Ciência e Inovação em Engenharia Mecânica e Engenharia Industrial Campus da FEUP, Porto, Portugal
[c] CMEMS – Center for MicroElectroMehanical Systems, University of Minho, Guimarães, Portugal

ARTICLE INFO

Keywords:
Aligned carbon nanotubes
Electrical anisotropy
Strain sensor
Multi-directional

ABSTRACT

In this work a new carbon nanotubes (CNT) based multi-directional strain sensor capable of quantifying and indicate strain direction is foreseen. This work investigates the electromechanical behavior of an aligned CNT sensing patch strained at 45° in order to validate its multi-directional sensing capability. Vertically aligned CNT forests are produced by chemical vapor deposition (CVD) and then mechanically knocked down onto polyimide (PI) films. Two configurations, diamond (D sample) and square (Sq sample), are considered. The relative electrical resistance ($\Delta R/R_0$) and the electrical anisotropy (R_B/R_A) upon strain increments are analyzed and compared to previous work results (0° and 90° strain direction). Both 45° samples, D and Sq, are sensitive to strain. A correlation between electrical anisotropy behavior and strain direction (0°, 45° and 90°) is established. The results show that with only an aligned CNT small patch it is possible to quantify and indicate strain in three directions.

1. Introduction

Nowadays, the use of carbon nanotubes (CNT) thin films for strain monitoring is quite common among researchers, due to CNT well-known electromechanical properties suitable for sensing applications, and its alignment has proven to facilitate some production processes of CNT based sensors (e.g., CNT forest embedded into polymeric matrices), and increased its sensitivity to strain [1]. Several methods are used for this alignment, such as electrical fields, assisted flow, mechanical stretching, direct draw from vertical forests and mechanical knock down, and all present its limitations and challenges. But, more importantly, the literature is quite limited regarding the actual strain monitoring itself. Most of the research [2–4] is focused on: strain quantification; sensitivity improvement; cyclic behavior; production process optimization, e.g., thin films with better CNT dispersion and without agglomeration; and only comprise one dimension (uniaxial) measurements. Even researchers that study the electrical behavior of CNT buckypaper based sensor at different strain angles [5], did not presented any distinctive direction indicator. Others [6] that studied the anisotropic electrical behavior of aligned CNT networks in two different directions, only explored the sensor electrical resistance individually without any strain direction indicator correlation. Recently, it has been reported [7] an anisotropic wearable sensor, however it had to incorporate two aligned patches to be able to indicate strain direction. Furthermore, commercially available strain gauges only measure strain in one direction.

To address this gap and as reported in our previous work [8], an aligned CNT based sensor for strain monitoring with a specific electrical characteristic, i.e., opposite electrical anisotropy behavior when strained at 0° and 90° regarding CNT alignment, which allows the sensor to indicate in which those directions the aligned sample is being loaded (bi-directional) and, simultaneously, quantify the strain value through the analysis of the electrical resistance. The applied deformation affects the CNT conductive network by affecting the electrons path and therefore the overall electrical resistance of the aligned sensor. Moreover, the electrical behavior depends on the CNT conduction mechanism that is dominant at each strain level: electron transfer by direct contact or tunneling effect [9,10]. When the sensor is strained at 0° regarding CNT alignment, a slippage between CNT happens and its electrical resistance varies linearly with the number of CNT-CNT junctions (N) being the direct contact the dominant conduction mechanism at small deformations. They are also inversely proportional, when the N increases the electrical resistance decreases and vice-versa. At higher strains, the distance between CNT overcome acritical value and the tunneling effect becomes dominant, therefore an electrical resistance exponential increase occurs. When the sensor is strained at 90° regarding its alignment, the CNT conduction is mainly done by tunneling effect and, thus, the

* Corresponding author.
E-mail address: b7525@dep.uminho.pt (A. Santos).

https://doi.org/10.1016/j.mseb.2022.115937
Received 27 October 2021; Received in revised form 23 May 2022; Accepted 9 August 2022
Available online 16 August 2022

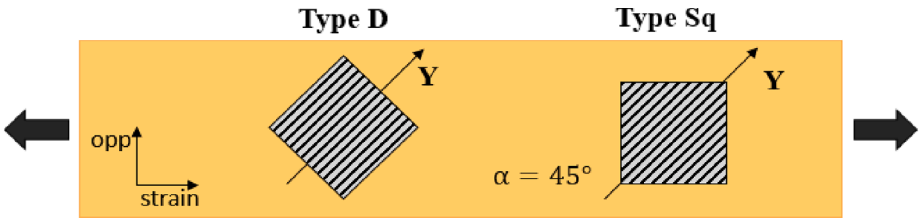

Fig. 1. Schematics of the two sensor configurations, type D and Sq, aligned at α = 45° regarding CNT alignment direction (Y), and its position regarding strain and opposite direction.

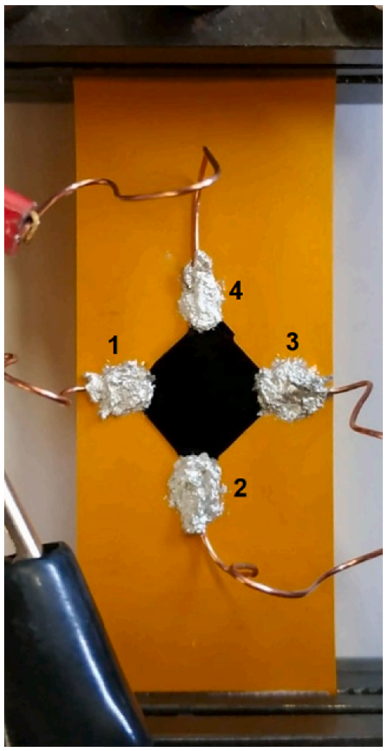

Fig. 2. Illustration of an aligned CNT strain sensor sample (diamond shape) with the positions of the four electrodes (1–4).

sensor presents an almost exponential increase in the electrical resistance upon strain increment. The quantification of the relative electrical resistance is used to infer strain sensitivity, Gauge factor (GF). Other important electrical property of the reported sensor is the opposite behavior of the electrical anisotropy, allowing the sensor to act as strain direction indicator.

In this work is reported an aligned CNT based strain sensor that is capable not only to quantify strain, but also to indicate three different strain directions (0°, 45° and 90°) with only a 10 mm × 10 mm sensing patch. Vertically aligned carbon nanotube (VA- CNT) forests were produced by chemical vapor deposition (CVD) and mechanically knocked down onto a polyimide film, using a metallic rod based apparatus. Two different aligned sensing patches configurations, diamond (D) and square (Sq), are considered. The D and Sq samples, were strained at 45° regarding CNT alignment and their relative electrical resistance and electrical anisotropy behavior upon strain increments are analyzed. Important to note that in a real monitoring application, it was thought that it would be quite interesting to study how the CNT conductive network would respond to 45° strain in different configurations. The results are promising and give a good contribute for the development of a multi-directional strain sensor that can quantify and indicate any strain direction with only a tiny square aligned CNT patch.

2. Materials and methods

2.1. Aligned CNT sensors production

VA-CNT forests were produced in a chemical vapour deposition (CVD) furnace at 750 ℃ with a gas mixture of helium/hydrogen/ethylene. These forests were mechanically knocked down and used in the strain sensors production. For this mechanical knock down, an apparatus composed by a metallic rod and two 3D printed supports were developed for this purpose. Detailed description can be found elsewhere [8].

In order to evaluate how an aligned CNT sensor would behave if strained at 45° regarding CNT alignment, two different geometric configurations were considered, diamond (D) and square (Sq) (Fig. 1), leading to two different production processes.

In type D configuration (Fig. 1), 10 mm × 10 mm VA-CNT forests were mechanically knocked down onto polyimide films, PI (75 μm Kapton MP film), with the diagonals of the aligned patch perpendicular to the faces of the film ensuring that the CNT patch is aligned at 45° in a diamond shape configuration. In type Sq configuration, 14 mm × 14 mm forests were mechanically knocked down, and a smaller square (10 mm × 10 mm) with CNT aligned at 45° were cut out. Both square patches were then transferred to PI films.

For the electrical resistance measurements, a silver conductive epoxy adhesive (8330S from MG Chemicals) was used as electrode of the CNT patches (Fig. 2).

2.2. SEM analysis

In order to evaluate the CNT alignment in the obtained forests and after the knock down process, a scanning electron microscopy (SEM) analysis was carried out in aNanoSEM-200 apparatus from FEI Nova.

2.3. Electrical resistance measurements

The produced aligned sensors, type D and Sq, were placed between two grips of the universal testing machine to perform the strain tests. The four electrodes (Fig. 2) were connected to an Arduino UNO and a laptop with the MATLAB control software in order to register the electrical resistance values simultaneously in two different directions, CNT alignment (Y-direction) and transversal directions (X) for the diamond shape sensor, whereas strain and opposite (opp) directions for the square shape sensor (Fig. 3, i) and ii), respectively).

The MATLAB software was developed from an adaptation of the Van der Pauw method, a four-point resistivity measurement method, for anisotropic conductors (different resistances in different directions) [8,11,12]. Briefly, adapt the calculations to anisotropic conductors, a conformal transformation was made resulting in Eq. (1), from which the $R_{A,\square}/R_{B,\square}$ value is obtained.

$$\frac{a/2}{b\sqrt{R_{A,\square}/R_{B,\square}}} = \frac{\int_0^{\pi/2} \frac{d\varphi}{\sqrt{1-k^2(\sin\varphi)^2}}}{\int_0^{\pi/2} \frac{d\varphi}{\sqrt{1-(\sin\varphi)^2+k^2(\sin\varphi)^2}}} \quad (1)$$

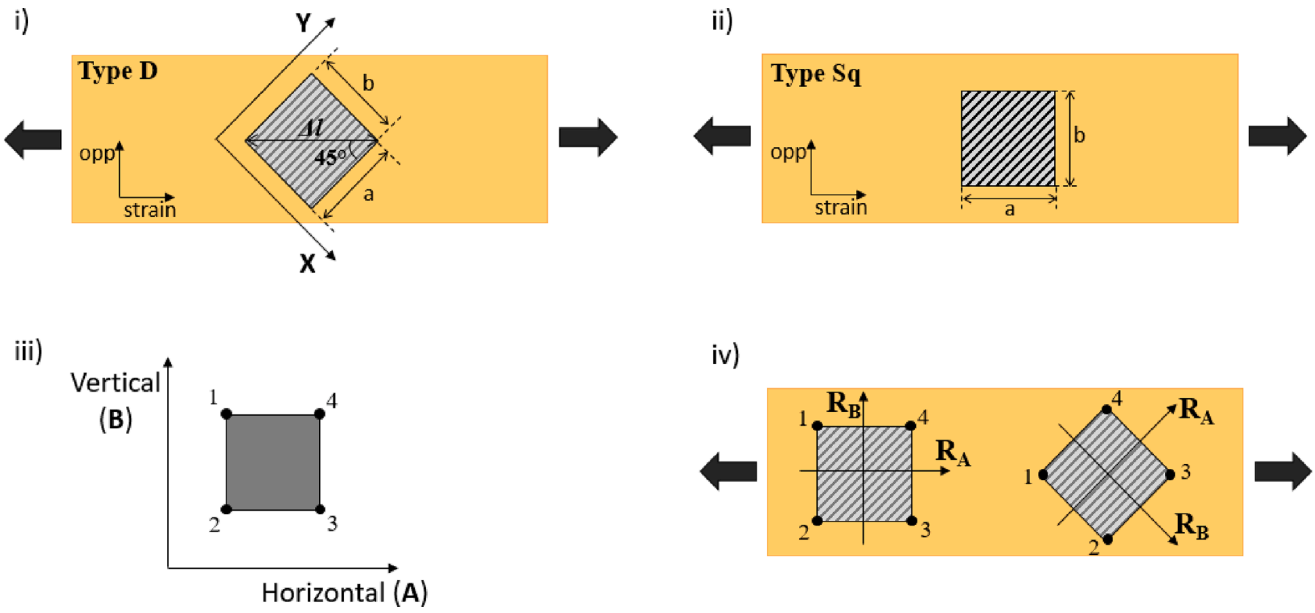

Fig. 3. Schematics of the two sensor configurations, i) type D with indication of longitudinal (Y) and transverse (X) direction regarding CNT alignment; ii) type Sq, both with strain and opposite (opp) direction, and dimensions patch (a and b) indication; iii) electrodes (1–4) position and A- and B-direction indication used in the experimental procedure; iv) electrodes (1–4) position and electrical resistance (R_A and R_B) direction indication for type D and Sq configurations.

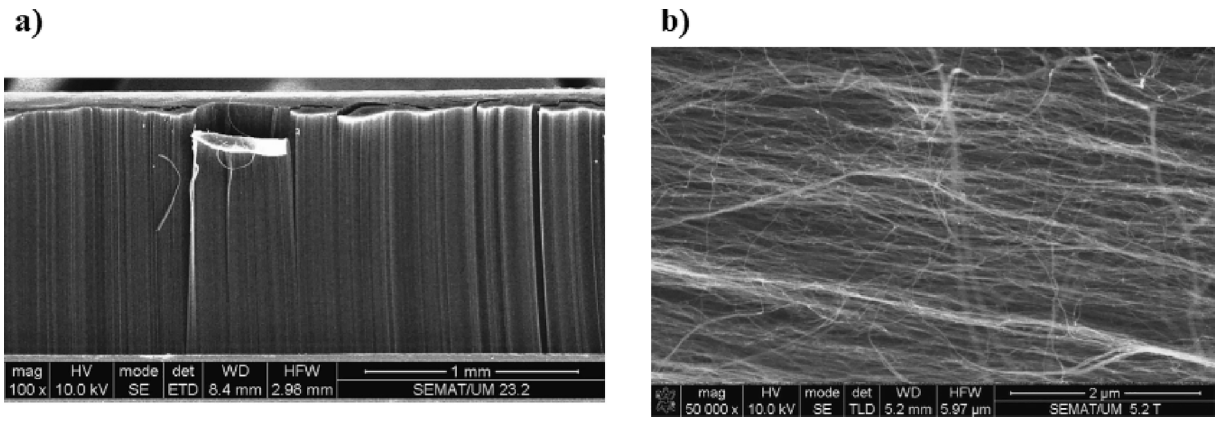

Fig. 4. SEM analysis of the VA-CNT, a), and the realigned sensor samples after the knock down process, b).

where *a* and *b* are the CNT's patch square dimensions, which initially are $a_0 = b_0 = 10$ mm. These dimensions will vary with the applied deformation during the tensile test. Specifically, in the case of the sensor type D (Fig. 3-iii)), $a = a_0 + \Delta l\cos 45^\circ$, and $b = b_0 + \Delta l\cos 45^\circ$, where Δl is the film elongation directly measured. In the case of the sensor type Sq (Fig. 3-ii)), $a = a_0 + \Delta l$ in the strain direction and $b = b_0 - \nu\varepsilon l_{t0}$ in the transverse direction, where ν is the Poisson ratio, ε is the mechanical strain and l_{t0} is the initial width of the PI film. $R_{A,\square}$ and $R_{B,\square}$ are the resistances in the two opposite directions (Fig. 3-iv)), and k is an experimental value which depends on the injected currents (I_{12} and I_{14}) and measured voltages (V_{43} and V_{23}). From an adaptation of the Van der Pauw equation [11], the sheet resistance value, R_s, is obtained:

$$e^{-\pi R_{vertical}/R_s} + e^{-\pi R_{horizontal}/R_s} = 1 \quad (2)$$

where, $R_{vertical}$ and $R_{horizontal}$ are the means of the experimental values of the electrical resistance in the A- and B-directions (Fig. 3-iii)), respectively.

Using the known Van der Pauw relation $R_{A,}R_{B,} = {R_s}^2$ and the $R_{A,}/R_{B,}$ value from Eq. (1), the resistances in the two different directions, $R_{A,} = R_A$ and $R_{B,} = R_B$ are obtained. In case of sensor type D (Fig. 3-i), iv)), $R_A = R_{YY}$ and $R_B = R_{XX}$, where R_{YY} and R_{XX} are the electrical resistances in direction of CNT alignment (Y-direction) and in the transverse one (X-direction), respectively. In case of sensor type Sq (Fig. 3-ii), iv)), $R_A = R_{strain}$ and $R_B = R_{opp}$, where R_{strain} and R_{opp} are the electrical resistances in strain direction and in the opposite one, respectively. These electrical resistance values were used to calculate the variations of the relative electrical resistance $R\text{-}R_0/R_0$, $\Delta R/R_0$, and the electrical anisotropy defined as the electrical resistance ratio (R_B/R_A), with the applied deformation during the tensile tests. Three and four samples of diamond and square shapes, respectively, were tested.

3. Results and discussion

3.1. SEM analysis

The CNT forests alignment and their realignment after the knock down process were assessed by SEM analysis. In Fig. 4 is shown the produced vertical aligned forests (a)) and the efficient realignment of the CNT in the direction of the knock down process (b)). More detailed characterization, Raman spectroscopy and transmission electron microscopy (TEM) analysis, of these forests can be found elsewhere [8].

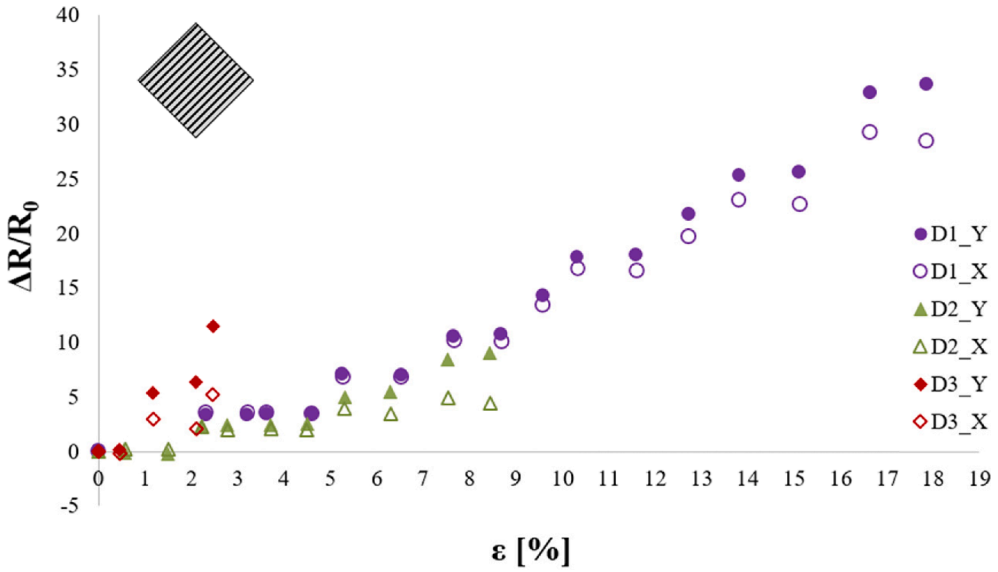

Fig. 5. Relative electrical resistance, $\Delta R/R_0$, of sensor type D (D1-D3) in longitudinal (Y) and transverse (X) direction regarding CNT alignment upon strain increments.

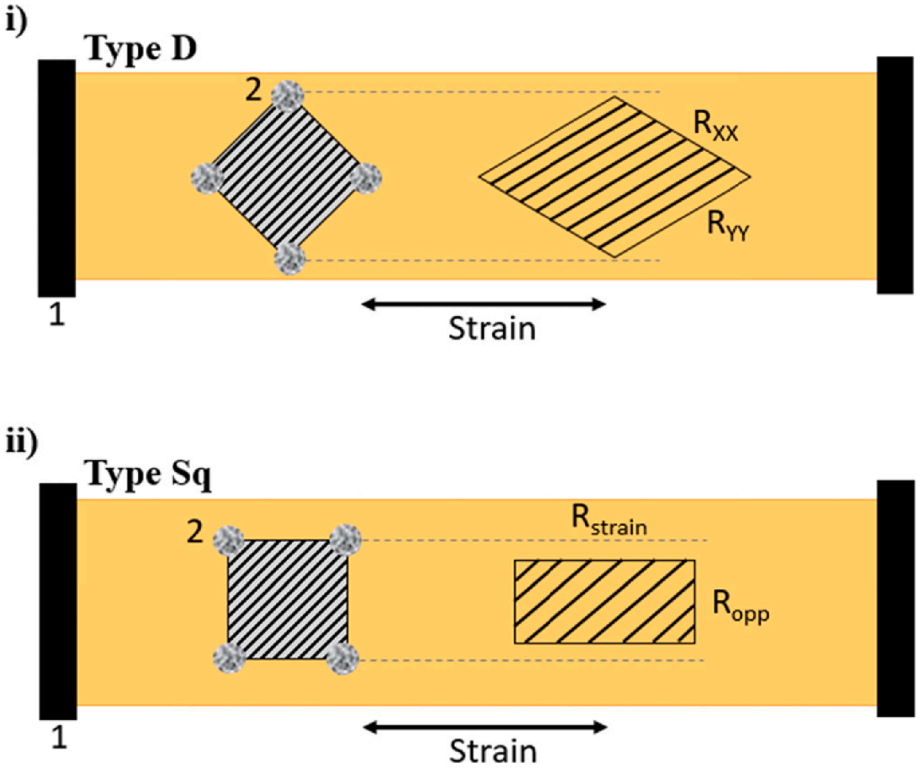

Fig. 6. Network deformation of the aligned CNT patch in two configurations: i) diamond (Type D) and ii) square (Type Sq) shape, grip (1) and electrodes (2) position.

3.2. Electrical resistance measurements

The CNT patches were strained in 45° regarding CNT alignment in two different configurations, type D and Sq (Fig. 1), and the relative electrical resistance ($\Delta R/R_0$) and anisotropy (R_B/R_A) behavior were analyzed.

3.2.1. Sensor type D – Diamond shape

Regarding sensor type D, all the samples (D1-D3) show an almost linear increase in the $\Delta R/R_0$ values with strain increments (Fig. 5), however one sample (D3) presents higher slope associated to a lower deformation at break meaning a higher decrease of the number of CNT-CNT junctions (N) with lower strain. Some results variability is observed due to samples production process. In Fig. 6-i), a CNT network deformation behavior is proposed for the diamond shape patch. When the two opposite diamond vertices are strained, the CNT are pulled apart and the number of CNT-CNT junctions (N) decreases, increasing the electrical resistance values in transverse (X) and longitudinal (Y) directions regarding CNT alignment (Fig. 5, blank (X) and full (Y) symbols). A mechanical restraint in the transverse direction (opp) was observed, meaning that the transverse deformation was not noticeable during the elongation of the sample, probably due to the aligned patch

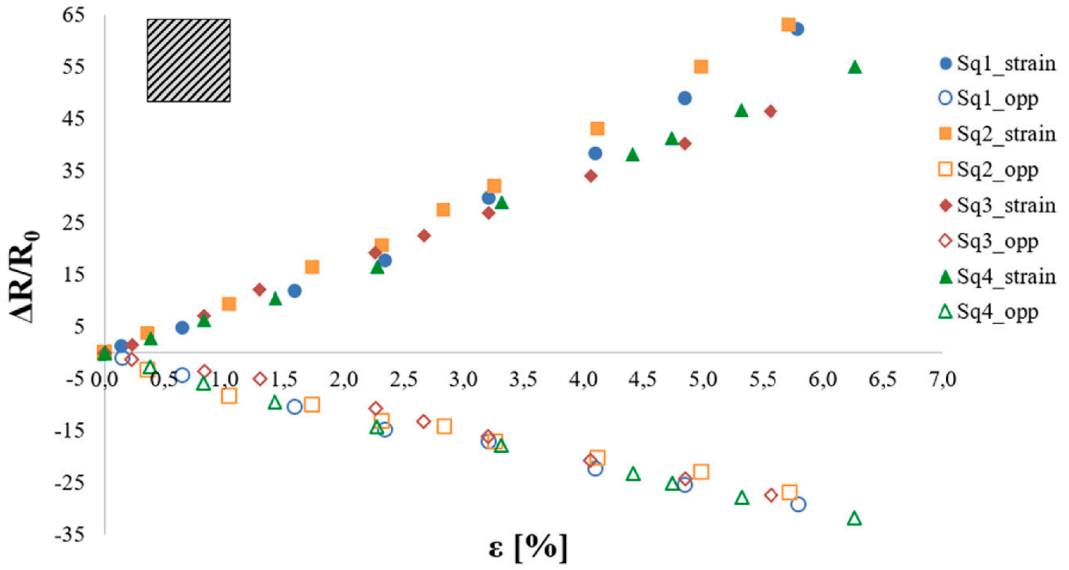

Fig. 7. Relative electrical resistance, $\Delta R/R_0$, of sensor type Sq (Sq1-Sq4) in strain and transverse (opp) direction upon strain increments.

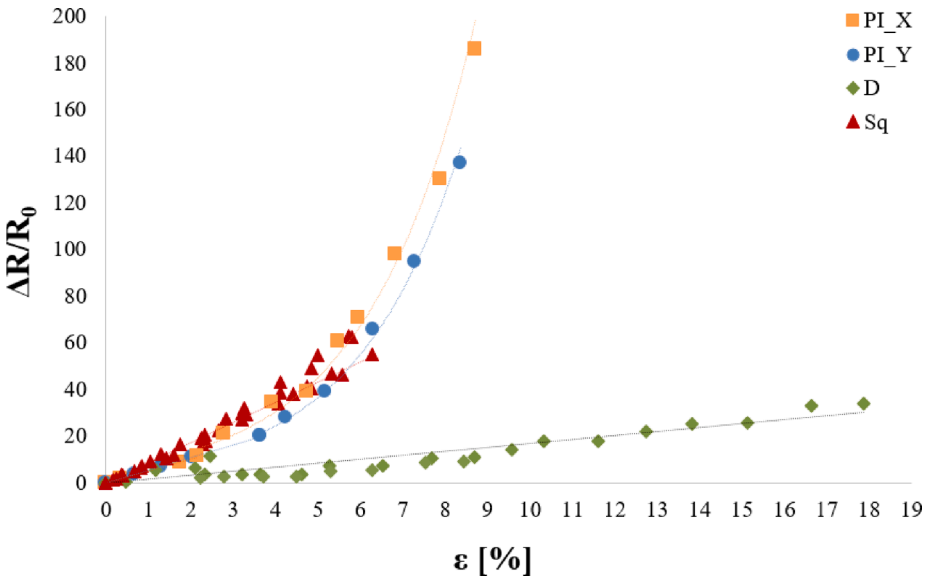

Fig. 8. Relative electrical resistance, $\Delta R/R_0$, of PI_X (90° strain direction), PI_Y (0° strain direction), D and Sq (45° strain direction) samples upon strain increments.

configuration (diamond), electrodes and grip position.

3.2.2. *Sensor type Sq – Square shape*

Regarding sensor type Sq, all the samples (Fig. 7), Sq1-Sq4, show a linear electrical resistance behavior upon strain increments. In the strain direction, the CNT are pulled apart and the number of CNT-CNT junctions (N) decreases leading to an increase of the $\Delta R/R_0$ value, whereas in the opposite direction, the CNT are slightly compressed and their number of junctions (N) increases leading to a decrease of the $\Delta R/R_0$ value. In Fig. 6-ii), a CNT network deformation mechanism is proposed for the square shape. When the square is strained at 45°, it suffers simultaneously a noticeable elongation and a small transversal compression (Poison ratio effect).

In Fig. 8, a comparison between the $\Delta R/R_0$ behavior of the samples PI_Y and PI_X (0° and 90° strain direction, respectively [8]), D and Sq (45° strain direction) is presented. All samples show a $\Delta R/R_0$ increase in the strain direction, due to the decrease of conductive paths in the aligned CNT network.

The D and Sq samples show a linear behavior due to the dominant conduction mechanism present: direct contact between CNT (CNT overlapping) promoted by a high CNT density [10]. When the sensor patch is strained at 45°, CNT slippage and overlapping occur and therefore their relative electrical resistance mainly depends on the CNT-CNT junctions, and varies linearly with the number of junctions (N) (equation (3)):

$$\frac{\Delta R}{R_0} = m\varepsilon \tag{3}$$

where m is a constant directly dependent on N.

The PI_X and PI_Y samples show both a similar mix conductive behavior, linear and non-linear, with $\Delta R/R_0$ increase upon strain increments in 90° and 0°, respectively, regarding CNT alignment. The conductive mechanism by CNT direct contact is dominant at small deformations, the $\Delta R/R_0$ increases linearly with N decrement during CNT-CNT slippage. However, after a critical strain value (ε_c) a non-linear $\Delta R/R_0$ increase is observed, as the CNT-CNT junction direct contact is lost,

Table 1
Relative electrical resistance ($\Delta R/R_0$) behavior, $\Delta R/R_0$ slope (GF) values and the respective numerical fitting of PI (PI_X and PI_Y), D and Sq samples.

Sample	PI				D	Sq
	PI_X		**PI_Y**			
Strain direction [°]	90		0		45	45
$\Delta R/R_0$ behavior	Linear ($\varepsilon \leq 2.16\%$)	Non-Linear ($\varepsilon \geq 2.16\%$)	Linear ($\varepsilon \leq 3.63\%$)	Non-Linear ($\varepsilon \geq 3.63\%$)	Linear	Linear
Fitting equation	$y = 5.58\varepsilon R^2 = 0.98$	$y = 6.69e^{0.39\varepsilon} R^2 = 0,98$	$y = 5.81\varepsilon R^2 = 0,99$	$y = 5.14e^{0.40\varepsilon} R^2 = 0,99$	$y = 1.69\varepsilon R^2 = 0,94$	$y = 9.82\varepsilon R^2 = 0,98$
Gauge Factor (GF)	5.58	21.3	5.81	16.4	1.7	9.8

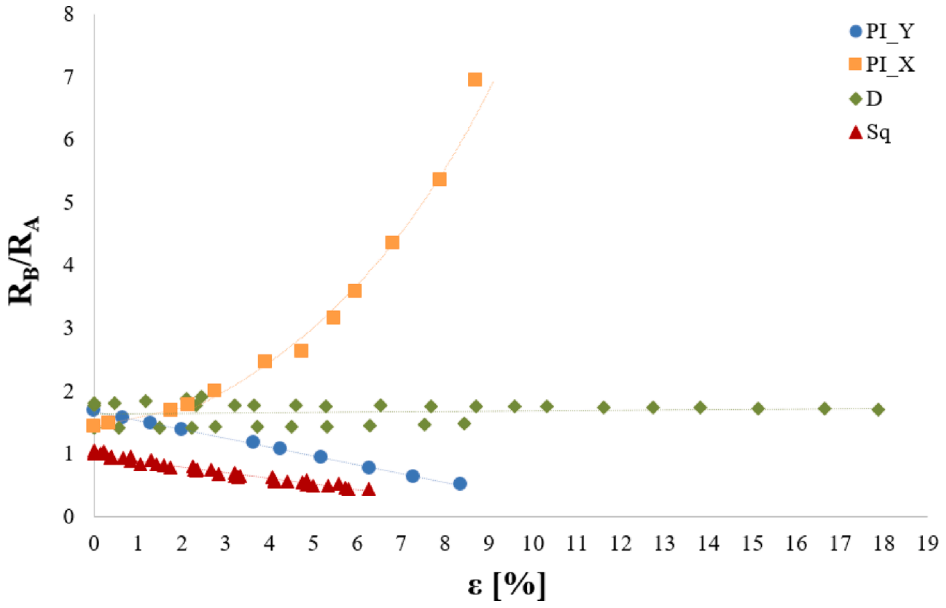

Fig. 9. Electrical anisotropy (R_B/R_A) vs strain (ε) for PI_Y (0° strain direction), PI_X (90° strain direction), D and Sq (45° strain direction) samples.

and the electrons transport within the aligned network is now mainly done by tunneling. As the strain increases, the CNT tunneling distance (d_{tun}) increases and the $\Delta R/R_0$ exponentially increases according to the tunneling effect model [5] described by $\frac{\Delta R}{R_0} = e^{2k(d_{tun}-d_0)} - 1$, where d_0 is the initial tunneling distance, k is a barrier junction constant and $d_{tun} \propto \varepsilon$. Therefore, a mix conductive model should be considered:

$$\frac{\Delta R}{R_0} \approx \begin{cases} m\varepsilon, \varepsilon \leq \varepsilon_c \\ e^{2k(d_{tun}-d_0)} - 1, \varepsilon > \varepsilon_c \end{cases} \quad (4)$$

The critical deformation point (ε_c), from which the tunneling effect becomes dominant, of the PI_Y sample ($\varepsilon_c = 3.63$) is higher than the PI_X sample ($\varepsilon_c = 2.16$) due to the differences in the CNT alignment. When the sensor is strained at 0° regarding CNT alignment (PI_Y), slippage between CNT occurs and CNT overlapping is maintained at higher strains compared to PI_X (90° strain direction). In Table 1, the $\Delta R/R_0$ behavior upon strain increment and numerical fitting of the results according to the mix conductive model (equation (4)) is presented. The results show a good accordance with the numerical fitting model with R^2 values between 0.94 and 0.99.

To assess the sensitivity to strain, the Gauge factor (GF), $GF = \frac{\frac{\Delta R}{R_0}}{\varepsilon}$, values were determined and their specific values presented in Table 1. For the linear region, the GF was calculated directly from the $\Delta R/R_0$ slopes, whereas for the non-linear region the GF was calculated using the $\Delta R/R_0$ maximum values. All the samples reached different GF values at different deformations at break. Considering the linear region, the GF values of PI_X (90° strain direction) and PI_Y (0° strain direction) samples are quite similar, lower than the ones of Sq samples but higher than the D samples GF values. However, the PI_X reaches the highest GF value in the non-linear region. When considering the specific deformation level, PI_Y, PI_X and Sq samples had similar and quite higher slope values compared to D samples, indicating a higher variation of the CNT conductive paths. The lower slope of D samples is due to the two converse effects that need to be considered in this sensor configuration: during straining the CNT are pulled apart decreasing N and increasing the electrical resistance value (dominant effect), however the CNT are simultaneously being pulled and realigned in the strain direction [13], increasing N and decreasing the electrical resistance. Therefore, $\Delta R/R_0$ slope of D samples is lower due to these compensating effects that result in lower variation of the number of junctions (N) in overall. Thus, the aligned CNT patch is suitable for strain quantification in the three different directions (0°, 90° and 45°), through relative electrical

Table 2
Electrical anisotropy (R_B/R_A) behavior and respective numerical fitting of the PI (PI_X and PI_Y), D and Sq samples.

Sample	PI			D	Sq
	PI_X		**PI_Y**		
Strain direction [°]	90		0	45	45
R_B/R_A behavior	Linear ($\varepsilon \leq 2.16\%$)	Exponential ($\varepsilon \geq 2.16\%$)	Linear	Linear	Linear
Fitting equation	$y = 0.15\varepsilon + 1.4$	$y = 1.09e^{0.20\varepsilon}$	$y = -0.14\varepsilon + 1.7$	$y = 0.005\varepsilon + 1.6$	$y = -0.09\varepsilon + 1$

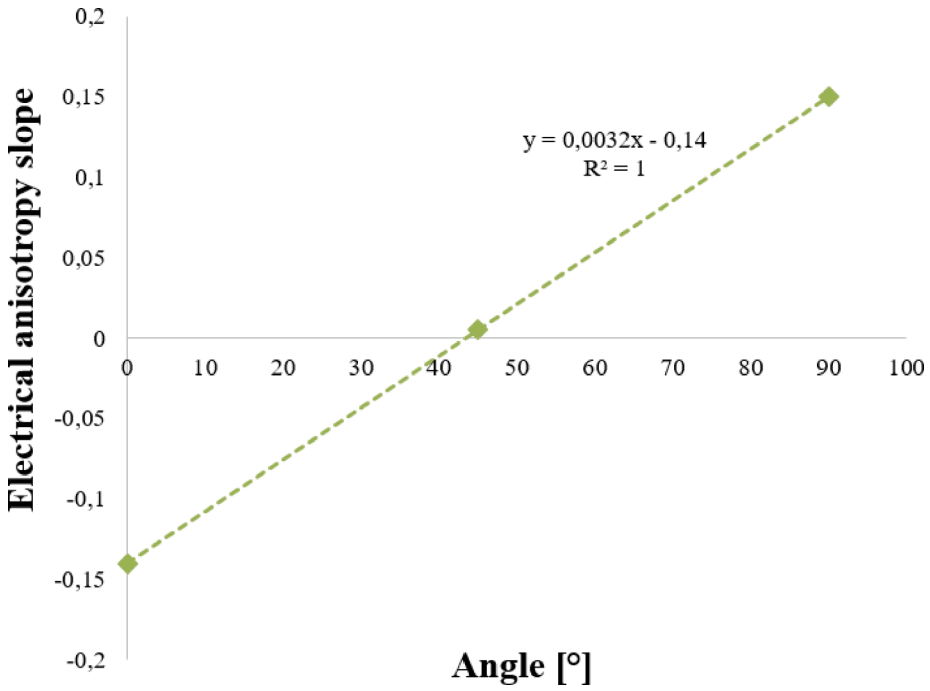

Fig. 10. Electrical anisotropy slope vs strain direction angle (°).

resistance measurements.

In Fig. 9, the electrical anisotropies (R_B/R_A) of PI_Y, PI_X, D and Sq samples are compared. Their electrical behavior, specific slope values and respective numerical fitting are presented in Table 2. Initially, the PI_X sample exhibits a linear positive slope and after a specific strain an almost exponential R_B/R_A increase can be observed. The PI_Y and Sq samples present a linear R_B/R_A decrease (negative slope) upon strain increments, whereas the D sample presents a lower slope of almost zero value. The D and Sq samples (45° strain direction) present a slope value between PI_Y (0° strain direction) and PI_X (90° strain direction) slope values. However, the Sq samples slope was close to the PI_Y value, not showing an electrical behavior as distinct as the D samples. These electrical behavior of PI_X, PI_Y and D samples prove that with just one aligned sensor can be used to infer different strain directions simultaneously. Moreover, the electrical anisotropy values do not show the variability observed for the $\Delta R/R_0$ values. Therefore, this unique behavior of the R_B/R_A at different strain directions (0°, 45° and 90°) is the fundamental point to infer strain direction with this aligned sensor:

$$\mathrm{R_B/R_A}\begin{cases} \textit{linear and negative slope} \rightarrow 0^{\circ}\ \textit{strain direction} \\ \textit{linear and} \approx \textit{zero slope} \rightarrow 45^{\circ}\ \textit{strain direction} \\ \textit{exponential and positive slope} \rightarrow 90^{\circ}\ \textit{strain direction} \end{cases}$$

In Fig. 10, it is shown the almost linear correlation ($R^2 = 1$) between the slope of the electrical anisotropy (R_B/R_A) with the strain direction angle (0°, 45° and 90°). With this relationship established between strain direction and anisotropy behavior, it has been shown that the developed aligned CNT patch based sensor is able to infer strain direction.

4. Conclusion

In this work, it was investigated how an aligned CNT strain sensor would behave if strained at 45° regarding its alignment, and how its behavior compares with 0 and 90° stretching. Two different sensor configurations, diamond (D) and square (Sq), are considered to study their influence on the CNT network deformation and conduction mechanisms. Their electrical behavior is compared with previously stablished relationships between the electrical anisotropy behavior and strain direction (0° and 90° regarding CNT alignment). Both 45° configurations show a linear increase in the $\Delta R/R_0$ values with strain increments, however D sample presents a lower slope, being less sensitivity to strain. This was attributed to two opposed effects: (i) the decrease of the number of CNT-CNT junctions (N) with deformation leading to an increment upon the electrical resistance; (ii) the realignment of CNT within the strain direction, increasing the number of CNT-CNT junctions (N) and decreasing the electrical resistance. The Sq configuration shows similar electrical behavior when compared to 0° and 90° deformed patches, although with a slight lower slope (i.e., GF).

The relationships between the electrical anisotropy and the strain direction (0°, 45° and 90° regarding CNT alignment) were also analyzed. Different slopes are evidenced from the different samples: 90° sample presents a positive slope, the 0° and 45° Sq samples show R_B/R_A decrement (negative slope) upon strain increments, whereas the 45° D sample evidence an almost zero slope value. A linear relationship was found between the R_B/R_A behavior and strain direction (0°, 45° D and 90°), that can be used as a strain direction indicator. While a commercial strain sensor has to be positioned in the direction that needs to be monitored, the aligned CNT based sensor reported in this paper can simultaneously give information regarding strain value and its direction from the electrical resistance values obtained from its four electrodes, regardless its positioning in the component. Therefore, it was shown that a small, aligned CNT sensing patch is suitable not only as a strain sensor, but also as strain direction indicator. The results presented are very promising and give a valid contribute to achieve a multi-directional sensor that simultaneously quantifies strain and indicates its direction with only a tiny sensing patch. However, further studies are needed to validate this sensor response in more strain directions.

Declaration of Competing Interest

The authors declare that they have no known competing financial interests or personal relationships that could have appeared to influence the work reported in this paper.

Acknowledgements

This work was partially funded under the project "IAMAT – Introduction of advanced materials technologies into new product development for the mobility industries", with reference MITP-TB/PFM/0005/2013, under the MIT-Portugal program exclusively financed by FCT – Fundação para a Ciência e Tecnologia. This work was also co-financed by national funds through FCT – Fundação para a Ciência e Tecnologia, with the scope of projects with references UIDB/05256/2020 and UIDP/05256/2020".

References

[1] O. Kanoun, C. Müller, A. Benchirouf, A. Sanli, T.N. Dinh, A. Al-Hamry, L. Bu, C. Gerlach, A. Bouhamed, Flexible carbon nanotube films for high performance strain sensors, Sensors. 14 (2014) 10042–10071, https://doi.org/10.3390/s140610042.

[2] A.I. Oliva-Avilés, F. Avilés, V. Sosa, Electrical and piezoresistive properties of multi-walled carbon nanotube/polymer composite films aligned by an electric field, Carbon N. Y. 49 (9) (2011) 2989–2997, https://doi.org/10.1016/j.carbon.2011.03.017.

[3] G. Yin, N. Hu, Y. Karube, Y. Liu, Y. Li, H. Fukunaga, A carbon nanotube/polymer strain sensor with linear and anti-symmetric piezoresistivity, J. Compos. Mater. 45 (2011) 1315, https://doi.org/10.1177/0021998310393296.

[4] A. Bouhamed, C. Müller, S. Choura, O. Kanoun, Processing and characterization of MWCNTs / epoxy nanocomposites thin films for strain sensing applications, Sensors Actuators A. Phys. 257 (2017) 65–72, https://doi.org/10.1016/j.sna.2017.01.022.

[5] T. Xu, Q. Qiu, S. Lu, K. Ma, X. Wang, Multi-direction health monitoring with carbon nanotube film strain sensor, Int. J. Distrib. Sens. Networks. 15 (2019). https://doi.org/10.1177/1550147719829683.

[6] A. Li, A.E. Bogdanovich, P.D. Bradford, Aligned Carbon Nanotube Sheet Piezoresistive Strain Sensors, Smart Mater. Struct. 24 (9) (2015) 095004, https://doi.org/10.1088/0964-1726/24/9/095004.

[7] J.-H. Lee, J. Kim, D. Liu, F. Guo, X.i. Shen, Q. Zheng, S. Jeon, J.-K. Kim, Highly aligned, anisotropic carbon nanofiber films for multidirectional strain sensors with exceptional selectivity, Adv. Funct. Mater. 29 (29) (2019) 1901623, https://doi.org/10.1002/adfm.201901623.

[8] A. Santos, L. Amorim, J.P. Nunes, L.A. Rocha, A.F. Silva, J.C. Viana, Aligned carbon nanotube based sensors for strain sensing applications, Sensors Actuators, A Phys. 289 (2019) 157–164, https://doi.org/10.1016/j.sna.2019.02.026.

[9] J. Lee, I.Y. Stein, M.E. Devoe, D.J. Lewis, N. Lachman, S.S. Kessler, S.T. Buschhorn, B.L. Wardle, Impact of carbon nanotube length on electron transport in aligned carbon nanotube networks, Appl. Phys. Lett. 106 (5) (2015) 053110, https://doi.org/10.1063/1.4907608.

[10] M. Park, H. Kim, J.P. Youngblood, Strain-dependent electrical resistance of multi-walled carbon nanotube/polymer composite films, Nanotechnology. 19 (5) (2008) 055705, https://doi.org/10.1088/0957-4484/19/05/055705.

[11] J.D. Wasscher, Note on four-point resistivity measurements on anisotropic conductors, Reports Philips Res. 16 (1961) 301–306.

[12] I. Kazani, G. De Mey, C. Hertleer, J. Banaszczyk, A. Schwarz, G. Guxho, L. Van Langenhove, Van Der Pauw method for measuring resistivities of anisotropic layers printed on textile substrates, Text. Res. J. 81 (20) (2011) 2117–2124, https://doi.org/10.1177/0040517511416280.

[13] Z. Tang, Q. Huang, Y. Liu, Y.i. Chen, B. Guo, L. Zhang, Uniaxial stretching-induced alignment of carbon nanotubes in cross-linked elastomer enabled by dynamic cross-link reshuffling, ACS Macro Lett. 8 (12) (2019) 1575–1581, https://doi.org/10.1021/acsmacrolett.9b00836.